Chemical wave front in two dimensions

A. Lemarchand, A. Lesne, A. Perera, and M. Moreau
Laboratoire de Physique Théorique des Liquides, Boîte 121, Université Pierre et Marie Curie, 4 place Jussieu, 75252 Paris CEDEX 05, France

M. Mareschal
Département de Chimie-Physique, Université Libre de Bruxelles, Campus Plaine, Boulevard du Triomphe, 1050 Bruxelles, Belgium
(Received 25 January 1993)

A reactive lattice-gas cellular automaton model is used to simulate a chemical wave front in two dimensions. The computed value of the front propagation velocity agrees with the one-dimensional (1D) theoretical value. In contrast, the front width is half the predicted 1D value. This result is explained by the fractal character of the interface. The fractal structure, described through several fractal dimensions, is shown to be independent of the reaction and diffusion parameter values.

PACS number(s): 47.70.Fw, 82.20.Mj, 82.20.Wt

A large variety of phenomena encountered in chemistry [1], biology [2], or materials science [3] are commonly described by nonlinear reaction-diffusion equations leading to complex space-time behaviors. Among these, wave-front propagation has been the subject of both theoretical and experimental interests. Much is known about propagating solutions in a one-dimensional (1D) medium [4–7]; it is easy to check that in a two-dimensional (2D) medium [8,9], proper 1D initial conditions will generate only effective 1D, macroscopic, and purely deterministic wave solutions.

In this Brief Report we shall introduce a lattice-gas model that provides a smaller scale description (referred to as "microscopic"), in order to investigate the validity of the macroscopic predictions when local microscopic and stochastic fluctuations are taken into account. This leads to macroscopic differences for the properties of the front, the origin of which is traced to the fractal character of the interface.

Let us consider the following reaction-diffusion equation first studied by Fisher [4] and Kolmogorov, Petrovsky, and Piskunov [5]:

$$\frac{\partial a}{\partial t} = ka(1-a) + D\left[\frac{\partial^2 a}{\partial x^2} + \frac{\partial^2 a}{\partial y^2}\right] . \tag{1}$$

In a chemical context, Eq. (1) describes a 2D chemical medium where two species A and B react according to the following autocatalytic scheme:

$$A + B \rightarrow A + A . \tag{2}$$

In Eq. (1), $a = a(x,y,t)$ denotes the local fraction of particles A, k is the rate constant, and D is the diffusion coefficient assumed to be identical for A and B. For sufficiently steep initial conditions independent of y (including the step function), 1D results [4–6] state that Eq. (1) admits uniformly translating solutions $a(x-ut)$, propagating in the x direction with the minimum allowed velocity $u_{\min}$,

$$u_{\min} = 2\sqrt{kD} , \tag{3}$$

and replacing the unstable uniform and stationary state $a \equiv 0$ by the stable state $a \equiv 1$. An approximate value s of the steepness at the inflection point can be used to define a front width [2] as:

$$e = \frac{1}{s} \approx 8\left[\frac{D}{k}\right]^{1/2} . \tag{4}$$

The 2D deterministic equation thus leads to a 1D front for initial conditions independent of y. However, a front propagation in a 2D lattice-gas cellular automaton (LGCA) cannot be reduced to an effective 1D problem. Thus, our first objective is to compare the theoretical results of the 1D deterministic front with the corresponding results deduced from the 2D simulation.

We consider a binary mixture in a Hardy–de Pazzis–Pomeau (HPP) model [10,11], with an equal number of particles A and B moving on a square lattice at integer times [note that the total number of particles remains constant under reaction (2)]. We choose units such that the lattice constant and velocity modulus equal 1. No more than one particle is to be found at a given time and node, moving in a given direction according to the so-called exclusion principle.

In order to ensure a steplike initial profile, the left (right) half of the lattice is filled with chemical species A (B) with a given number density ρ. A two-step cellular-automaton updating rule is defined on the Boolean field of node states. Step 1 is propagation along the direction of particle velocities. In contrast with previous approaches [12], step 2 is a momentum-conserving collision. All different configurations, including those obtained by permutation of the different chemical species, are considered for collisions between two, three, and four particles. When several post collision configurations are possible, the final state is randomly chosen. For every collision between particles of different species, the collision is reactive with a probability K linked to the rate con-

TABLE I. Comparison between the minimum propagation velocity u_{min} predicted by the deterministic 1D theory and the mean velocity $\bar{u}$ deduced from the 2D simulation for different values of rate constant k and diffusion coefficient D.

D	1.42	2.25	2.25	2.25	4.75	8.08
k	0.01	0.01	0.02	0.04	0.01	0.006
u_{min}	0.24	0.30	0.42	0.60	0.44	0.44
$\bar{u}$	0.24	0.32	0.45	0.57	0.44	0.44

stant k of reaction (2).

Following Kapral and co-workers [12], we have checked that these collision rules lead to the relation $k=K\rho$. A careful test has proven that the system, in a statistically stationary state, obeys the usual mean-field description [13]. The diffusion coefficient for our model verifies [14] that $4D=(2/\rho)-1$. Classical periodic boundary conditions are imposed only in the y direction. The propagation of the front is taken into account in the following manner: Defining a lattice column by the set of nodes with an identical abscissa x, we couple the first and the last columns but keep them separated by a permeable wall. If a particle A from the first column crosses the wall, it changes into a particle B —reciprocally for a particle B moving from the last column into the first one.

In order to mimic an infinite medium in the x direction, it is necessary to counterbalance the consumption of particles B due to reaction (2). When the number of particles A becomes greater than half the total number of particles, the wall is translated to the left and all the lattice is updated, the excedent of A being converted into B.

The wall motion contains global information about the entire front propagation and the front velocity is identified with the wall velocity. Its time-averaged value $\bar{u}$ is computed for different values of k and D. In Table I we compare $\bar{u}$ with (3). The agreement is satisfactory, indicating that in a 2D microscopic and stochastic medium, an initial step-function profile evolves to a front propagating with the minimum velocity as in 1D macroscopic [6] or microscopic [7] media.

Figure 1 represents the mean concentration profiles of A and B in the wall frame after averaging over y and t. In Table II the mean front width $\bar{e}$ is compared to the macroscopic value (4). As opposed to the previously obtained 1D simulation results [7] we find here that $\bar{e}$ and e do not coincide. Rather, we get $\bar{e}=e/2$.

TABLE II. Variation of front properties with the rate constant k for a fixed diffusion coefficient $D=2.25$. e and $\bar{e}$ are the front widths deduced, respectively, from the 1D theory and the 2D simulation; F_1 (F_2) is the fractal dimension of the interface from Fig. 3(a) [Fig. 3(b)]; and S is the statistical entropy.

k	0.003	0.006	0.01	0.02	0.04
e	219	155	120	85	60
$\bar{e}$	103	76	57	43	29
F_1	1.63	1.64	1.63	1.62	1.51
F_2	1.91	1.91	1.89	1.80	1.68
S	0.681	0.681	0.681	0.679	0.678

A closer analysis of the microscopic interface between the reactive species A and B thus appears necessary. A recent analysis of a purely diffusive phenomenon [15] suggests an investigation of possible fractal characteristics of the front. We define the interface as the set of lattice sites occupied by two different species. An instantaneous plot is displayed in Fig. 2. A mere observation reveals a spatial extension and an asymmetrical distribution of points in the x direction: The 2D interface is somewhat more spread to the left, similarly to the 1D front profile [7].

To be more quantitative, we implemented three different definitions of the fractal dimension. They are based upon different theoretical characteristics of fractal sets of points extended in a computational form to "real" fractals; these are defined, rather, as sets of cells of finite size linked to the resolution of the lattice model. The asserted fractal character of the interface is proved by a self-similarity test, performed by computing the dimension of the structures deduced after contraction of the lattice constant by a reasonable factor; we chose here 4 and 8. A cell of the contracted lattice is considered as an interface point as soon as the corresponding 4×4 (8×8) square of the initial lattice contains at least 1 (2, in order to reproduce a decrease of sensitivity) interface point(s). In Figs. 3(a) and 3(b), the curves corresponding to the initial and contracted lattices have identical slopes equal to a well-defined fractal dimension, independent of the chosen lattice constant, thus having an intrinsic, hence relevant, meaning. Figure 3(a) illustrates the box-

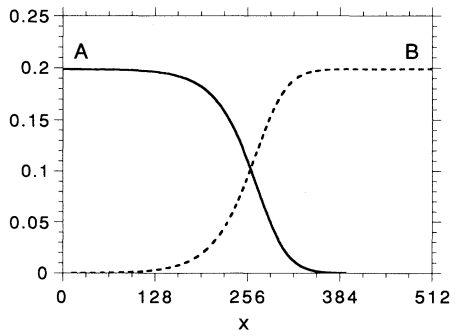

FIG. 1. Mean front profiles in the wall frame for the following conditions: 512×512 lattice, rate constant $k=0.003$, and diffusion coefficient $D=2.25$.

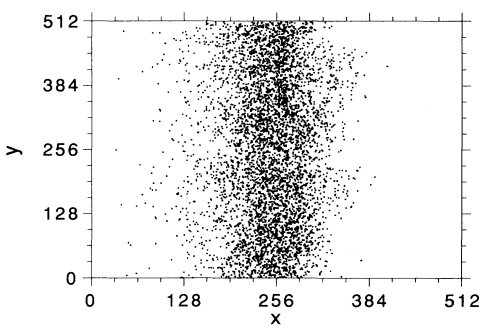

FIG. 2. Interface, defined as the lattice nodes occupied at the same time by the two reactive species A and B, for the conditions in Fig. 1.

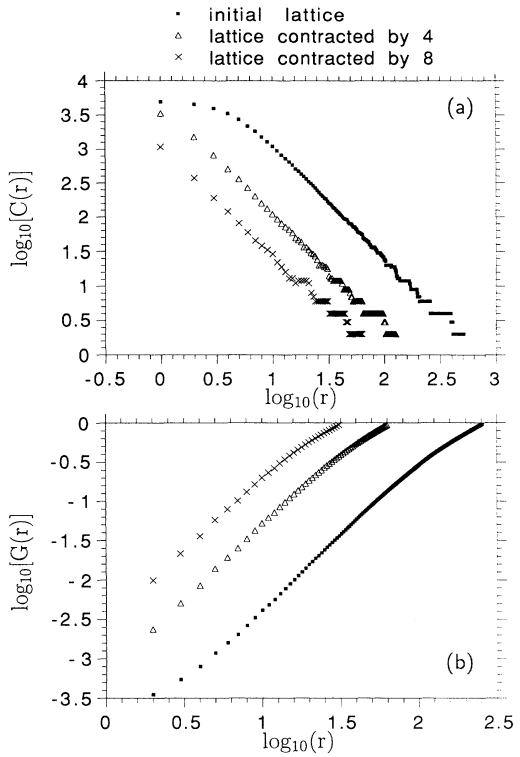

FIG. 3. Self-similarity test and determination of the fractal dimension of the interface in Fig. 2 for (a) the box-counting method [log-log plot vs r of the number $C(r)$ of square boxes of side r required to cover the interface] and (b) the Grassberger and Procaccia method [log-log plot vs r of the mean number $G(r)$ of interface points in a disk of radius r around an interface point]. The slope of the linear region yields the fractal dimension.

counting method [16]. The dimension value denoted by $F_1 \approx 1.63 \pm 0.02$ appears to be independent of k and D, as can be seen in Tables II and III. Quite similar results have been obtained using the alternative codimension method [16]. The first method leads to the so-called "similarity dimension," the second one to a "coverage" dimension (or capacity). A somewhat larger value $F_2 \approx 1.89 \pm 0.02$ is found using the Grassberger and Procaccia method [17] illustrated in Fig. 3(b). We believe that this last method, initially designed to compute the dimension of a strange attractor from a generic trajectory, overestimates in our case the dimension; indeed, points of the interface inner region should not be given the same reactive weight, as they are less accessible than the points of the outer region of the interface. The discrepancy between F_1 and F_2 reveals, in addition, a tangled and intricate structure rather than a diffuse and fingerlike structure. We define the statistical entropy S of the interface as

$$S = -\left[\frac{1}{p}\right] \sum_{i=1}^{p} [a_i \ln(a_i) + b_i \ln(b_i)] ,$$

where p is the number of interface points and a_i (b_i) the fraction of particles A (B) at node i. In Tables II and III we show that S is independent of the values of k and D, thus supporting the universality of the fractal properties.

TABLE III. Variation with the diffusion coefficient D of the statistical entropy S and of the fractal dimensions F_1 and F_2 for a fixed rate constant $k = 0.01$.

D	1.42	2.25	4.75	8.08
F_1	1.38	1.63	1.61	1.63
F_2	1.91	1.91	1.85	1.80
S	0.673	0.681	0.687	0.689

Finally, the dimension F_x (or F_y) of an interface section at fixed x (or fixed y) is computed. Very close values $F_x \approx F_y \approx 0.82 \pm 0.02$ are found, indicating that the fractal structure is isotropic, and self-similar rather than self-affine (though directions x and y are not equivalent).

The above discussion can be used to show why the fractal nature of the mesoscopic interface gives $\bar{e} \approx e/2$. The boundaries $\alpha \approx 10$ and $\beta \approx 70$ of the linear regime in Fig. 3 are identified with the smallest and the greatest scales for which the fractal properties are significant. We denote $C(r)$ the number of $r \times r$ cells covering the interface. From the very definition of F_1, we have

$$C(\alpha) = \left[\frac{\beta}{\alpha}\right]^{F_1} C(\beta) . \tag{5}$$

At the macroscopic scale β ($\beta > \alpha$), the fractal details are not detectable, and it is relevant to identify the perceived interface area $\beta^2 C(\beta)$ with the reactive surface eL of the deterministic plane front, where L is the lattice extension in the y direction. At the microscopic scale α, the interface area $\alpha^2 C(\alpha)$ is equal after a space-time average to $\bar{e}L$; since the fractal structure increases the chemical efficiency of each site, this effective area is smaller than the macroscopic one eL. Equation (5) leads to the quantitative estimate of this reduction:

$$\bar{e} = e\left[\frac{\alpha}{\beta}\right]^{2-F_1} , \tag{6}$$

which gives $\bar{e} \approx e/2$, as is observed in Table II. Detailed aspects of these investigations will be presented in a forthcoming article.

In conclusion, the lattice-gas simulation of a wave front propagating into an unstable state has shown that the propagation velocity is selected in a 2D microscopic and stochastic medium exactly as in a 1D macroscopic and deterministic one. But the profile width is decreased by a factor of 2. This result is justified by the fractal nature of the interface, which increases the reactivity of each site. The fractal properties appear to be independent of the reaction and diffusion parameters and allow us to give a quantitative estimation of the width decrease.

This work was partially supported by NATO CRG 920083. The Laboratoire de Physique Théorique des Liquides is "Unité de Recherche Associée au CNRS No. 765."

[1] F. Baras and D. Walgraef, editors, *Nonequilibrium Chemical Dynamics: From Experiment to Microscopic Simulations,* special issue of Physica A **188** (1992).
[2] J. D. Murray, *Mathematical Biology* (Springer, Berlin, 1989).
[3] *Nonlinear Phenomena in Materials Science II,* edited by G. Martin and L. Kubin, Solid State Phenomena Vol. 23/24 (Trans Tech Publications, Zurich, 1992).
[4] R. A. Fisher, Ann. Eugenics **7**, 335 (1937).
[5] A. Kolmogorov, I. Petrovsky, and N. Piskunov, Bull. Univ. Moscow. Ser. Int. Sec A **1**, 1 (1937).
[6] D. G. Aronson and H. F. Weinberger, Adv. Math. **30**, 33 (1978).
[7] A. Lemarchand, H. Lemarchand and M. Mareschal (unpublished).
[8] M. Bramson, P. Calderoni, A. de Masi, P. Ferrari, J. Lebowitz, and R. H. Schonnmann, J. Stat. Phys. **45**, 905 (1986).
[9] P. Clavin, P. Lallemand, Y. Pomeau, and G. Searby, J. Fluid Mech. **188**, 437 (1988).
[10] J. Hardy, O. de Pazzis, and Y. Pomeau, Phys. Rev. A **13**, 1949 (1976).
[11] U. Frisch, D. d'Humières, B. Hasslacher, P. Lallemand, Y. Pomeau, and J. P. Rivet, Complex Systems **1**, 649 (1987).
[12] A. Lawniczak, D. Dab, R. Kapral, and J. P. Boon, Physica D **47**, 132 (1991).
[13] C. R. Doering and D. Ben-Avraham, Phys. Rev. Lett. **62**, 2563 (1989).
[14] P. M. Binder, Complex Systems **1**, 559 (1987).
[15] H. Z. Cao, J. R. Hardy, R. W. Douglass, P. T. Dawkins, and S. R. Dunbar, Phys. Rev. A **45**, 3841 (1992).
[16] K. R. Sreenivasan, Annu. Rev. Fluid Mech. **23**, 539 (1991).
[17] P. Grassberger and I. Procaccia, Phys. Rev. Lett. **50**, 347 (1983).